Iranian Journal of Science and Technology, Transactions of Civil Engineering (2023) 47:105–118
https://doi.org/10.1007/s40996-022-00915-9

RESEARCH PAPER

Rocking Motion of a Mid-Rise Steel Plate Shear Wall on Foundation–Soil Medium

J. Mirlohi[1] · P. Memarzadeh[1] · F. Behnamfar[2] · M. Bayat[1]

Received: 23 January 2022 / Accepted: 18 June 2022 / Published online: 9 July 2022

Abstract

In the concept of conventional structural design, the general assumption is that the structure is fixed at its base, while the fact is that the supporting soil medium allows for some general motions of the foundation due to its flexibility. Regardless of stiffness of structure's frames, this phenomenon results in a subsequent increase in natural period of the system and alters the overall expected response. Moreover, considering soil–structure interaction (SSI) in dynamic analysis of a building structure may result in producing an additional motion of the structure due to rocking motion of the building. The main purpose of the current study is to explain how the mechanism of the effect of rocking motion on the behavior of a steel plate shear wall (SPSW) structure. In this order, the SSI phenomenon is studied and explained in a typical mid-rise steel plate shear wall frame resting on shallow foundation. The SSI effects on the inelastic responses of such a frame due to El Centro 1940 earthquake were examined in detail using a direct method, and also, the results were compared to those for the fixed base frame. Then, a procedure is presented to clarify how SPSW behavior could be influenced by rocking component. Here, two site conditions were considered (typical stiff and soft soil deposits). The results indicated that the SSI greatly affects the seismic performance of the SPSW structure in terms of the seismic story shear forces, displacements and story drifts.

Keywords Rocking motion · Steel plate shear wall · Soil–structure interaction · Direct method

1 Introduction

Steel plate shear wall (SPSW) is a lateral load resisting system widely used in buildings. The SPSW consists of a vertical infill plate connected to the surrounding beams and columns (Liu et al. 2020a; Wang et al. 2021). An accurate analytical model for SPSW building structure needs to study the effect of all components such as the structure, foundation and subsoil, regarding the interaction between them. Practically, in conventional design, the frame is presumed to be fixed at its base, but in reality it rests on soil (Bai et al. 2021; Shabanlou et al. 2021). Vibration energy of the structure is transmitted to the soil strata and dissipated; thus, in addition to soil material hysteresis damping, the radiation damping is also caused due to wave propagation. Moreover, soil as a flexible medium can influence the overall stiffness of the structure. This effect depends on the dominant period of input ground motion as well as the structure and subsoil characteristics such as their stiffness ratio. Structures on the soft soils undergo larger soil–structure interaction (SSI) effects than those resting on stiff soils (Carbonari et al. 2008; Liang et al. 2018; Choudhury et al. 2019; Gharad and Sonparote 2019; Kamgar et al. 2020; Motallebiyan et al. 2020; Bahuguna and Firoj 2021). For example, Dicleli & Karalar (2009) indicated that the influence of SSI on the fundamental vibration period of bridges is not considerable for stiff soil conditions but became more important in the case of softer soil conditions. Liu et al. (2020b) based on both shaking table and numerical simulation stated that the effects of SSI are more important when the frequency of soil and structure are closer. The effects of SSI could be briefed through the following phrases: reduction of the natural frequency of structure; increase in damping; decrease of the story shear forces; and influence on the drifts (Kramer 1996; Dutta et al. 2004; Ghandil and Behnamfar 2017; Choudhury et al. 2019; Kamgar et al. 2021). The performance-based earthquake engineering encourages incorporation of

✉ P. Memarzadeh
p-memar@iaun.ac.ir

[1] Department of Civil Engineering, Najafabad Branch, Islamic Azad University, Najafabad, Iran

[2] Department of Civil Engineering, Isfahan University of Technology, Isfahan, Iran

soil–foundation nonlinearity and energy dissipation in order to reduce structural force demand (Raychowdhury 2011; Tavakoli et al. 2020), noting that neglecting SSI may result in over- or under-estimation of the responses.

Among numerous investigations on the effect of SSI on the behavior of different types of structures (such as braced, moment resisting (El Ganainy and El Naggar 2009; Tabatabaiefar and Massumi 2010; Raychowdhury 2011; Shirzadi et al. 2020), steel shear walls (Kamgar et al. 2019; Kamgar and Babadaei Samani 2022) and concrete shear wall (Oliveto and Santini 1993; Carbonari et al. 2008; Jayalekshmi and Chinmayi 2016) frames), no study was found in this regard for the SPSW structures. The main objective of this article is to study the seismic performance of a typical mid-rise SPSW structure, incorporating SSI effects. For this purpose, the direct method was adopted to model the soil domain. Numerical modeling of the system was carried out with a finite element method (FEM), using Abaqus software.

Despite mentioned studies, there are limited studies on the importance of nonlinear SSI and its impact on seismic behavior of a SPSW, as a structure generally stiffer than the moment-resisting frames and more ductile than the bracing systems. This paper is dedicated to clarify and to explain a possible mechanism by which a mid-rise SPSW behavior is influenced by the rocking component. In this order, an applicative example of SSI problem using FEM is presented. A time direct method was used to investigate nonlinear behavior of SPSW with an equivalent-linear model for underneath soil deposit during time history analyses. Two soil types (i.e., type II and type IV) have been studied.

2 Properties of SPSW Building Considered

A typical mid-rise SPSW building designed by Sabelli and Bruneau (2006) according to AISC 341-10 - American Institute of Steel Construction (2010) for the lateral earthquake forces specified by ASCE-7 (2000) was considered for the current study.

The SPSW was a 9-story, 3-bay frame with infill plates in the second bay's panels. The geometry and section properties of the SPSW structure are presented in Fig. 1. The x-translation inertia due to floor masses w 5440 kips (2468 ton) in total, distributed equally among the first to ninth floors.

Imperial	SI
W27*94	W690*140
W30*108	W760*161
W30*116	W760*173
W14*283	W360*421
W14*398	W360*592
W14*665	W360*990

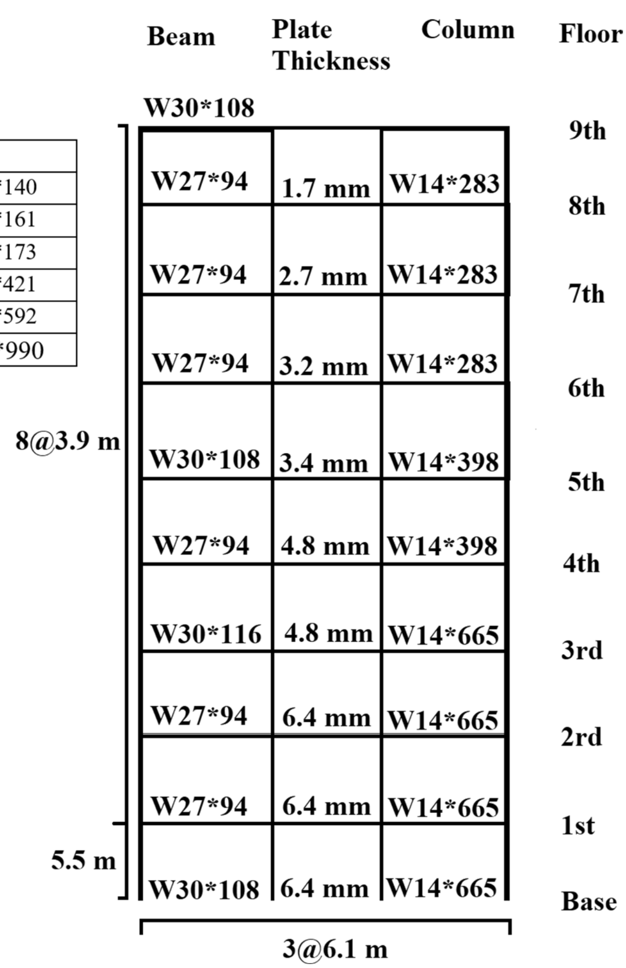

Fig. 1 Dimensions and properties of SPSW building (Sabelli and Bruneau 2006)

3 Modeling

The development of the SPSW model in Abaqus and verification of its validity are described in (Memarzadeh 2008; Memarzadeh et al. 2010). The beams and columns are modeled by use of the 2-node finite beam element (B31) with linear interpolation formulations in three dimensional space. Also, the 4-node doubly-curved shell element (S4) is used to model the web plates. This element uses linear interpolation, full integration, and thick shell theory for finite membrane strains and arbitrary large rotations.

Extensive sensitivity analysis and convergence studies have been performed on different modeling parameters such as the linear bulk viscosity parameter, the number of thickness Gauss integration points, as well as the degree of mesh, which can be found in (Memarzadeh et al. 2010). Accordingly, totally 25 section points are specified to be used for integration over the beam and column sections; 9 points in web, 9 in each flange. Also, seven Gaussian integration points through the thickness of the shell elements are used. A mesh of 20 by 13 elements (20 elements over the width of the shear wall) is used to model the infill plates except for the first story infill plate which has a mesh of 20 by 18 elements. The length of the beam elements is selected to match the mesh size in the infill plates.

Previous studies indicated that modeling of infinite soil medium plays a vital role in soil–structure interaction (Çelebi et al. 2012; Edip et al. 2017; Hökelekli and Al-Helwani 2020; Homaei and Yazdani 2020; Jiao et al. 2021). The unbounded nature of the soil medium requires a special boundary condition that does not reflect seismic waves into the soil–structure domain. Various models of boundary condition exist that allows for energy transmission. The wave energy is absorbed through the special boundary conditions like the transmitting, non-reflecting and silent boundaries. Since, in this work, parallel to vertical springs have been used and distributed vertical dashpots were also included to account for the radiation damping in soil (Madani et al. 2015; Behnamfar and Banizadeh 2016). The non-reflecting viscous boundaries developed by Lysmer and Kuhlemeyer (1969) and White et al. (1977) are widely applied in various dynamic soil–structure interaction problems.

Abaqus provides infinite elements that are based on Lysmer and Kuhlemeyer (1969) for dynamic response. These elements were used in conjunction with standard finite elements, which model the area around the region of interest, with the infinite elements that model the far-field region. Infinite elements provide a quiet boundary to the finite element model in dynamic analysis. In this study, the radiation condition was treated by the infinite elements implemented in Abaqus. Here, three-dimensional, reduced integration, eight-nodded solid continuum elements (C3D8R) have been used for finite element modeling of foundation and soil (light gray in Fig. 2) and three-dimensional, eight-nodded solid continuum infinite elements (CIN3D8) have been utilized to simulate the far-field region (dark gray in Fig. 2); the mesh density of the infinite elements was much coarser than that of the internal soil.

The local viscous boundaries should be placed far away from the structure in order to obtain realistic results; therefore, the horizontal distances between the soil boundary and center of the structure are assumed to be 192 ft. (57.60 m), 3 times of foundation length from each side. The reason for assuming this distance is to reach the free-field motion

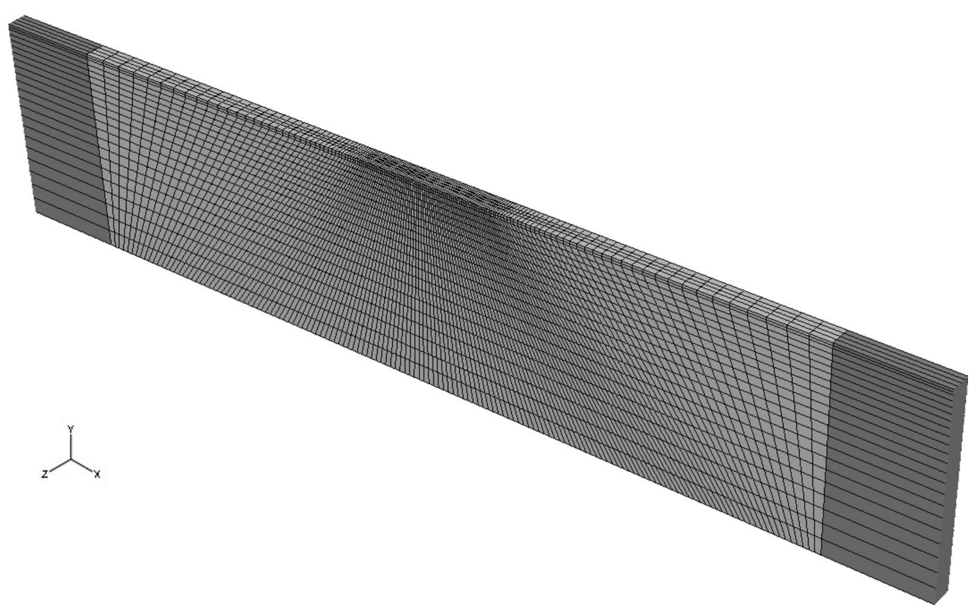

Fig. 2 Coupled finite–infinite element and unbounded domain idealization of soil

Table 1 Geotechnical characteristics of the subject soils

Soil type	Shear wave velocity (m/s)	γ (KN/m^3)	Poisson's ratio
II	518	20	0.30
IV	131	18	0.40

Table 2 Dynamic properties of soils

Soil type	Shear modulus ratio (G/G_{max})	Damping (%)
II	0.91	4.9
IV	0.55	9

of ground surface after deconvolution, similar to El Centro earthquake record. Bed rock depth is assumed to be 100 ft. (30 m) for all considered soil types. The soil element size is small at the footing and gradually increases toward the external boundaries of the soil (Figs. 2, 4). The infill plate and columns of SPSW are assumed to be supported by shallow strip foundations. The foundation dimension is 768 × 40 in. (19.2 × 1 m.) in plan, while a depth of embedment of 30 in. (0.75 m) is provided. These dimensions were determined on the basis of Terzaghi's bearing capacity formula for strip footings with an ultimate bearing capacity of 334 kPa with a factor of safety of 3.0 (Herrmann and Bucksch 2014). The numerical model uses the explicit central difference time integration rule for dynamic analysis. The related formulation can be found in Memarzadeh (2008).

4 Material Properties

In order to investigate the effect of SSI on the seismic behavior of SPSW, two types of soil deposits with different shear wave velocity (V_S) profiles are used in this study, namely: soil type II (stiff soil); and soil type IV (soft soil) in accordance with the site classification of Iranian Standard No. 2800-05 (Abkar and Lorki 2011). The structures with soil type II ($375 < V_S < 750$ m/s) and IV ($V_S < 175$ m/s) represent systems with small and large SSI effects, respectively. Therefore, these two extreme cases can cover most of the SSI problems in earthquake engineering practice. Characteristics of the subject soils are shown in Table 1. The dynamic properties of soils are shown in Table 2.

The soil dynamic response is nonlinear even at low to moderate deformation levels, during seismic events; therefore, soil nonlinearity should be appropriately taken into consideration. In this study, equivalent-linear properties are used to take into account approximate soil nonlinearities. These properties are obtained through 1-D wave propagation analyses conducted through the program SHAKE (Ordonez 2007). The method used in this program assumes horizontally layered deposits and vertically propagating shear waves. The nonlinearity of soil behavior is known very well thus most reasonable techniques to provide reasonable estimates of ground response that is very challenging issue in civil engineering. In the current study, equivalent linear approach was used to evaluate ground surface motions which was implemented in widely accepted ground response software SHAKE and widely used for site response analysis. The SHAKE program conducts a series of analyses on an iterative basis, such that at every time step, the values of secant shear modulus and equivalent linear damping ratio are updated to correspond to the current shear strain value to incorporate approximate soil nonlinearities. Viscous damping is imposed on soil material in numerical simulations using Rayleigh damping based on Eq. (1) in order to approximate the inherent energy dissipation mechanisms due to the soil hysteresis damping.

$$C = \alpha M + \beta K \tag{1}$$

where C, M and K are damping, mass and stiffness matrices, respectively. To calculate the coefficients α and β, equivalent linear damping ratio was assumed for the first two modes of the system. The foundation was assumed to experience linear elastic behavior under seismic shaking.

Material properties of the structural members and the infill plates have the following specifications (Sabelli and Bruneau 2006):

$$\begin{aligned} &E_1 = 29{,}000 \text{ ksi (200 GPa)}, \quad E_2 = 290 \text{ ksi (200 MPa)}, \\ &\nu = 0.3, \quad \rho = 489 \text{ lb/ft}^3 (7.8 \text{ ton/m}^3), \\ &F_{yp} = 36 \text{ ksi (248 MPa)}, \quad F_{yb} = 50 \text{ ksi (345 MPa)} \end{aligned} \tag{2}$$

where E, ν and ρ are Young's modulus, Poison's ratio and density of steel material, respectively; F_{yp}, F_{yb} are the steel plate and boundary member yield stresses, respectively. The assumed stress–strain correlations of the steel plate, beam and column materials are expressed in Fig. 3.

5 Dynamic Analysis of Soil–Structure Interaction

The structure was modeled on soil types of II and IV; first with the soil as flexible base and then as fixed base structure without soil being denoted as the Reference SPSW from here on. Accordingly, earthquake record was applied to the system in two different ways. For modeling soil and structures together (flexible base), the earthquake record was applied to the combination of soil and SPSW directly. Figure 4 shows the generated mesh for the SPSW with soil in direct method.

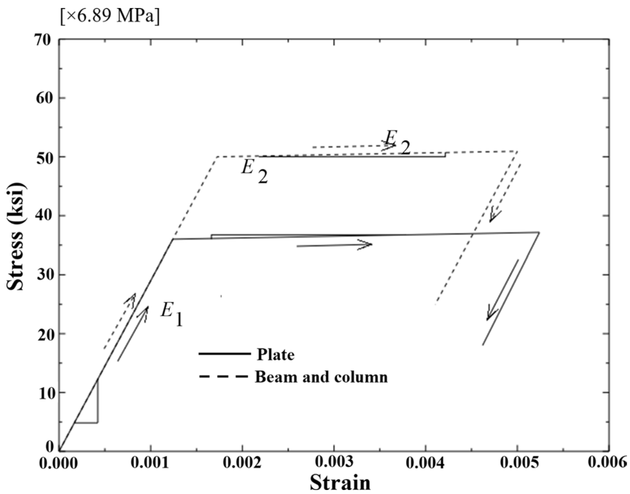

Fig. 3 The assumed stress–strain relationship of the material (Sabelli and Bruneau 2006)

A zoom-in figure of the in-fill plate mesh can be found in Memarzadeh et al. (2010).

For modeling the structures as fixed base, the earthquake record was applied directly to the base of the structure; here, the structure was assumed without soil. The results obtained from flexible base condition were compared with the ones obtained from Ref. SPSW (fixed-base condition). For this purpose, a ground motion record, the N–S component of the 1940 El Centro earthquake with maximum amplitude of 0.319 g was selected for dynamic analysis. Table 3 indicates some relevant information of the given record.

As the seismic signal was recorded on the ground surface, in reality the motion of the base rock (to which the soil–structure system will be subjected) should be obtained by deconvolution. The program SHAKE (Ordonez 2007) was used to conduct a deconvolution analysis in order to obtain the base motion that corresponds to the above ground motion for each soil type.

In order to verify the soil width, as shown from Fig. 5, acceleration time history of ground surface after

Table 3 Characteristics of El Centro earthquake

Earth-quake	Station	Record/com-ponent	PGA(g)	PGV (cm/s)	PGA/PGV (1/s)
El Centro, 1940	USA	El Centro/N–S	0.319	36.1	8.6

deconvolution far enough from SPSW was computed by Abaqus for both the soil types. Figure 6 shows the El Centro earthquake and ground motion record after deconvolution for comparison. As can be noticed, the response is almost the same with the El Centro earthquake record, demonstrating that the size of 3-D model of soil and the boundaries are in agreement with the incident wave defined at the outcropping bedrock using program SHAKE (Ordonez 2007).

6 Validation of the Finite Element Model

6.1 Experimental Natural Frequency

Rezai (1999) conducted ambient vibration and impact tests in the University of British Columbia (UBC) on a four-story steel plate shear wall frame during the shake table test to obtain the natural frequency of vibration. Figure 7 illustrates the experimental test specimen and its numerical model built in the present study.

Figure 8 compares the experimental and numerical results for the natural frequency of the four-story SPSW. As seen, there is a relatively good agreement between the results.

6.2 Energy Balance

Energy output is particularly important in checking the accuracy of the solution in an explicit dynamic analysis. Figure 9a illustrates the energy time histories for the entire SSI model of the 9-story SPSW. All the energy time histories mentioned in Fig. 9a has been defined in Memarzadeh et al. (2010). As

Fig. 4 Generated mesh of SPSW with soil in direct method (flexible base)

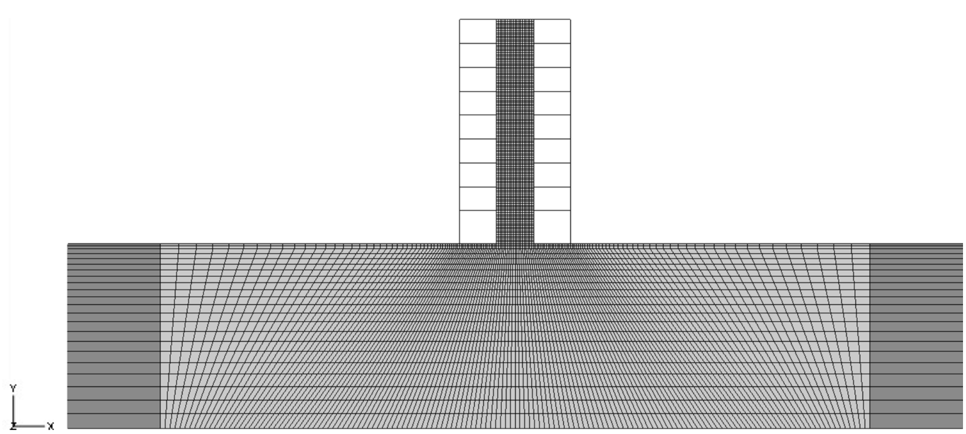

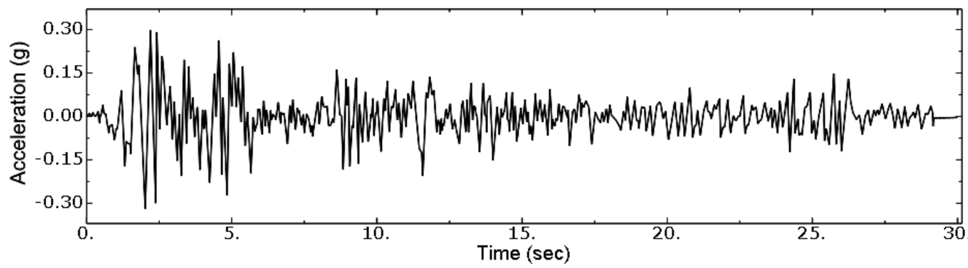

Fig. 5 Accelerogram of El Centro earthquake, 1940, N–S component

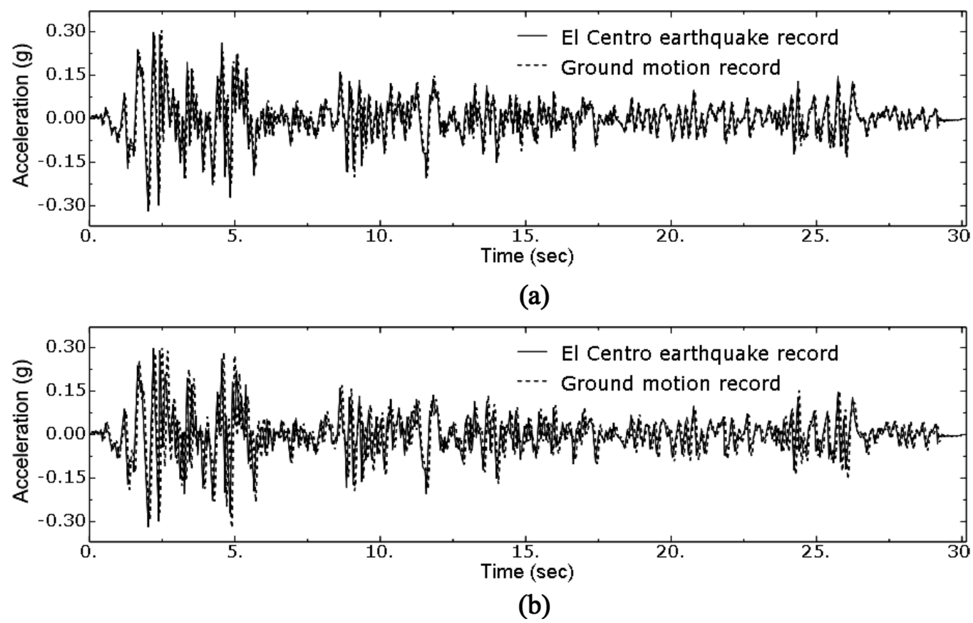

Fig. 6 Ground motion record after deconvolution for **a** soil type II and **b** soil type IV

shown in Fig. 9a, the artificial strain energy of the model was negligible compared to that of the input energy. Also, it was found that the total energy of the system vanishes over the time, i.e., the energy balance was obtained. These observations imply that the accuracy of the solution is acceptable. It is observed in Fig. 9a that almost all of the supplied energy to the SSI system is dissipated by viscous damping as expected due to the effect of solid medium infinite elements (i.e., viscous boundary) and hysteretic material damping. The energy time history for Ref. SPSW is illustrated in Fig. 9b for comparison.

6.3 Resonant Structural Deformation

In order to evaluate the validity of the model, the finite element model of the coupled soil–structure systems was subjected to a sinusoidal force at the roof level of models with a 0.9043, 0.5487 and 0.3492 Hz frequency equal to the first vibration of modes Ref. SPSW, SPSW founded on soil type II and soil type IV, respectively, for a time interval of 10 s. Afterward, it was allowed to vibrate freely for 20 s. The lateral displacements of some floors of SPSW with all the different base conditions (fixed and flexible) are shown in Fig. 10. According to these figures, a resonance in the first 10-s interval is observed that is followed by a decrease of the free vibration amplitudes due to function of the damping.

It can be deduced from Fig. 10 that the dynamic SSI leads to an increased attenuation of the floor response which is related to an important characteristic of SSI (i.e., energy dissipation by means of hysteretic material damping and radiation damping). Thus, a significant part of the vibration energy of the SSI system may be dissipated either by radiation waves, emanating from the vibrating foundation–structure system back into the soil, or by hysteretic material damping in the soil.

7 Results

The seismic response of the structure in terms of the story displacements and drifts as well as story shear are selected as response parameters of interest, since these are generally considered the most important response parameters to evaluate the seismic vulnerability of a structure in seismic design practice. The results of SSI models will be compared

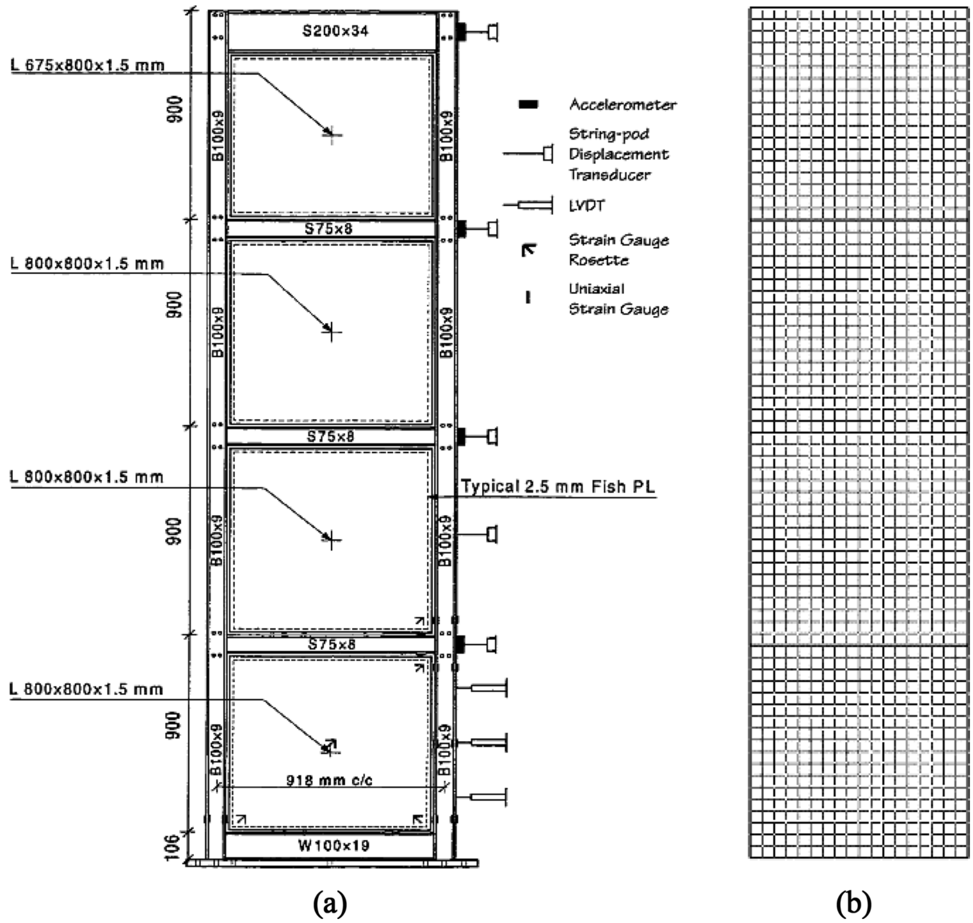

Fig. 7 Four-story SPSW frame **a** tested by Rezai (1999); **b** modeled by Abaqus

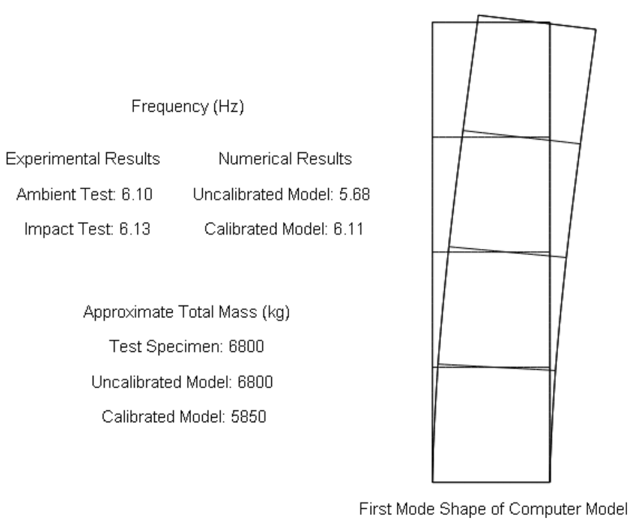

Fig. 8 Experimental and numerical results for natural frequency of 4-story SPSW

to those obtained from Memarzadeh et al. (2010). The status of plastic areas in the in-fill plates of Ref. SPSW at the termination time instance of dynamic analysis can be found in Memarzadeh et al. (2010).

7.1 Natural Frequencies

The SSI effects on natural frequencies are evaluated by means of an eigenvalue extraction performed on (Memarzadeh et al. 2010) and current SPSW models (without and with considering SSI effect, respectively). The change in frequencies of the first four modes due to the effect of SSI is studied on SPSW resting on each soil type. Table 4 indicates the four lowest natural frequencies and corresponding mode shapes of the SPSW frame over a range of soil types and the four natural frequencies of Ref. SPSW (Memarzadeh et al. 2010) pointing out the percentage differences obtained for all soil types as well. A maximum decrease of about 6% is found for SPSW resting on soft soil, while the minimum reduction is observed to be around 7% for SPSW resting on stiff soil.

As shown in Table 4, the natural frequency of the SPSW decreases with increasing softness of supporting soil. As known, supporting soil medium allows for some general motion of the foundation due to its flexibility. This

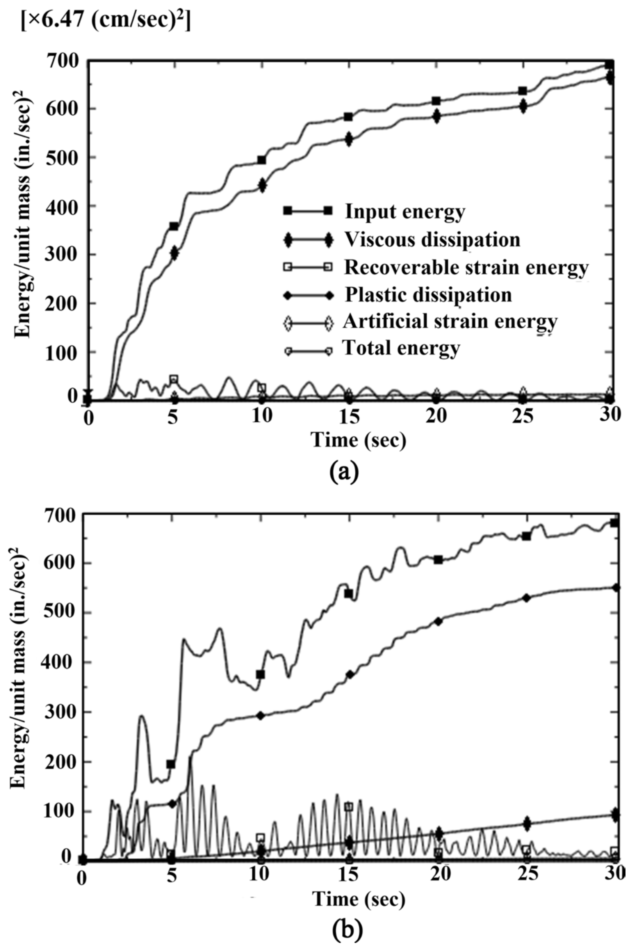

Fig. 9 Energy time histories of the entire model: **a** SSI model (soil type IV), **b** Ref. SPSW

phenomenon reduces the overall stiffness of the building frames resulting in a subsequent increase in the natural periods of the system that is one of the most important effects of SSI. Since the SPSW exhibits great changes in natural frequencies due to the effect of SSI, significant change is expected to be found in their seismic response due to the effect of SSI.

Table 5 shows the modal mass participation ratios of the three modes of SPSW with fixed or flexible base. As can be seen, the modal mass of the first 3 modes participates in the 95.8% and 88.4% of the total response of the SPSW with fixed base and the SPSW on the Soil type II, respectively.

7.2 Story Displacement and Drift

Structural displacement is an important parameter in prediction of structural damage. The floor displacements relative to the base are obtained by subtracting the base displacement from the absolute floor displacements. The response envelopes of relative displacements and drift ratios (story drift to story height) are illustrated in Fig. 11a for the SPSW with different base conditions. It is observed that the story displacement increases as much as 60% and 240% for SPSW founded on stiff and soft soil, respectively, as the base condition changes from fixed to flexible. The increase is greatest for soil type IV. As shown in Fig. 11b, the story drifts of SPSW with flexible base increase from 77 to 245% in the case of soil type IV. The results clearly point out that the story drift and deflection increase with decreasing the shear wave velocity of the soil deposit. The increase in story deflections occurs due to the reduction in the global stiffness resulting from the induced soil–foundation flexibility. It is also noted in Fig. 11a that the structure shows vibration in its fundamental mode; this indicates that the higher modes contribute to the selected SPSW and ground motion insignificantly.

It is worth mentioning that with respect to (Memarzadeh et al. 2010), the story drift ratio is distributed more evenly throughout stories in SSI models, particularly when the building frame is considered to be resting on soil type IV.

7.3 Story Shear

Story shear is another important parameter from the structural designers' point of view. The variation of change in story shear due to the incorporation of soil flexibility as compared to the same value obtained at fixed-base condition, expressed as a ratio of such response of SSI models to Ref. SPSW, is plotted in Fig. 12. Comparing the results obtained from the SSI models and Memarzadeh et al. (2010) reveals that story shear may reduce significantly due to soil flexibility with respect to Memarzadeh et al. (2010) particularly for the soft soil. It is observed that the ratios of story shear incorporating SSI to that of Memarzadeh et al. (2010) are less than 1.0 in all stories for both types of soil. Therefore, the story shear forces of structures modeled as flexible base are always less than the story shear of structures modeled as fixed base. These results are in good agreement with Seismic and Provisions (1997). This clearly implies the importance of considering SSI in order to obtain good predictions of the shear response.

7.4 Foundation Rocking Effects

As known, there is a direct relationship between story shear forces and story drifts in common practice structural analysis of fixed-base frames. Then, it is expected that a decrease in story shear results in decrease of corresponding story drift and vice versa. However, in SSI analysis of the SPSW structure, as seen in Figs. 11b and 12, the story shear forces and corresponding drifts are related inversely. This observation has been also reported by other researchers (El Ganainy and El Naggar 2009; Tabatabaiefar and

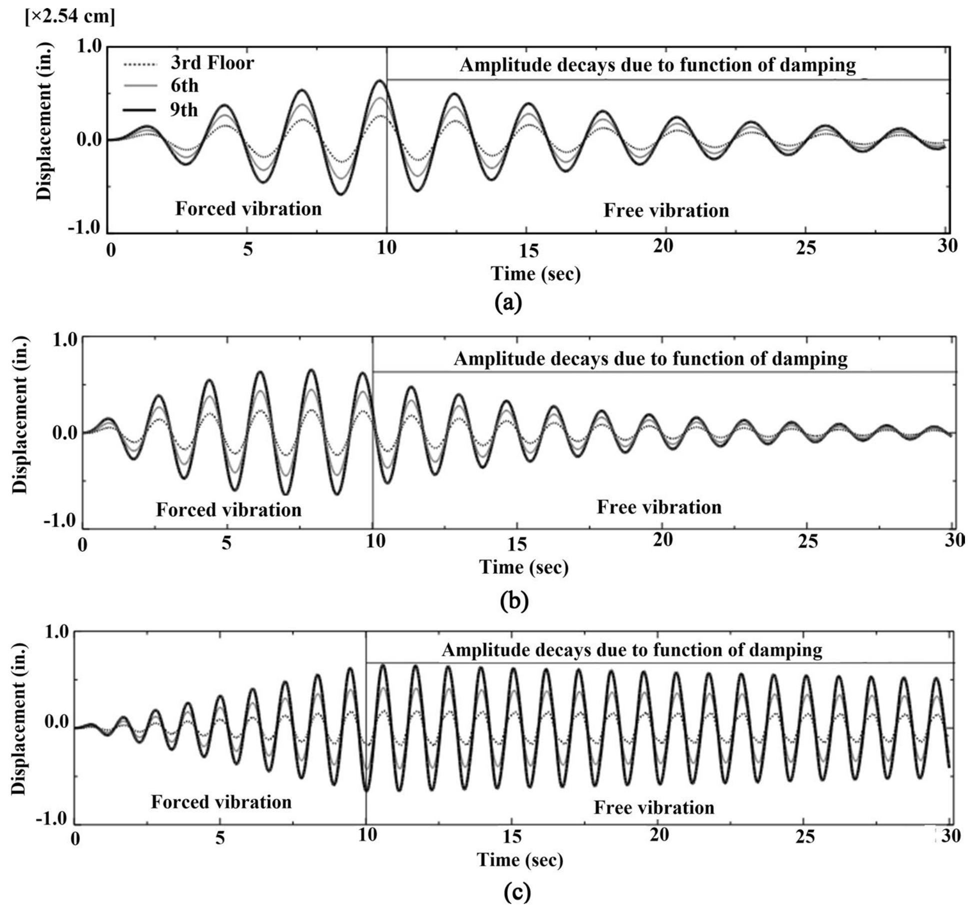

Fig. 10 Lateral displacement of floors in SPSW with: **a** flexible base (soil type IV), **b** flexible base (soil type II), **c** fixed base (Memarzadeh et al. 2010)

Table 4 Mode shapes and natural frequencies of the SPSW

Mode shape	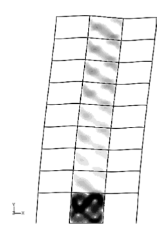		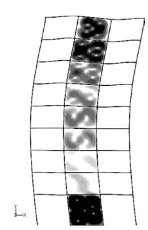		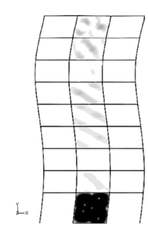		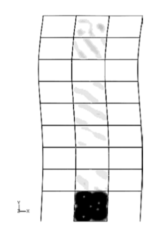	
	1st mode, difference		2nd mode, difference		3rd mode, difference		4th mode, difference	
	(Hz)	(%)	(Hz)	(%)	(Hz)	(%)	(Hz)	(%)
Ref. SPSW (Sabelli and Bruneau 2006)	0.9043	00.00	2.7761	00.00	4.9129	00.00	5.1586	00.00
SPSW on soil II	0.5487	− 39.32	2.5676	− 07.51	4.2517	− 13.46	4.8039	− 06.87
SPSW on soil IV	0.3492	− 61.38	2.3500	− 15.35	3.4736	− 29.30	4.4015	− 14.67

Massumi 2010; Raychowdhury 2011) and recently justified by the fact of the foundation rocking motion, without providing any derivation in detail. Hence, this section is going to devote its attention to describe the reason for this observation and derive it.

As known, a building structure resting on flexible medium such as soil may experience rocking motion at its base due to ground motion, while this motion never occurs in fixed-base buildings. The horizontal lateral displacement of a floor

Table 5 Modal mass participation ratios of the three modes of SPSW with fixed or flexible base

Floor number	First mode vector		Second mode vector		Third mode vector	
	Ref. SPSW	SPSW on soil II	Ref. SPSW	SPSW on soil II	Ref. SPSW	SPSW on soil II
9	0.543575	0.525169	0.496443	0.55032	0.460316	− 0.21678
8	0.492037	0.476425	0.25862	0.324735	− 0.04623	− 0.55028
7	0.42526	0.419334	− 0.01746	0.064498	− 0.42016	− 0.51781
6	0.351898	0.358459	− 0.25026	− 0.16506	− 0.42503	− 0.21678
5	0.280441	0.297919	− 0.39126	− 0.32134	− 0.15574	0.089958
4	0.212086	0.236154	− 0.43375	− 0.39012	0.157765	0.303663
3	0.150534	0.176281	− 0.39579	− 0.38542	0.366225	0.354566
2	0.096328	0.117409	− 0.30892	− 0.32735	0.410837	0.284794
1	0.046695	0.05915	− 0.17439	− 0.22166	0.27700	0.16719
Modal mass participation ratio (%)	75.04	78.99	16.45	8.44	4.34	1.01

Fig. 11 Response envelopes of **a** floor displacements relative to foundation; and **b** story drift for Ref. SPSW (line) and SSI models (dashed) as % of total height

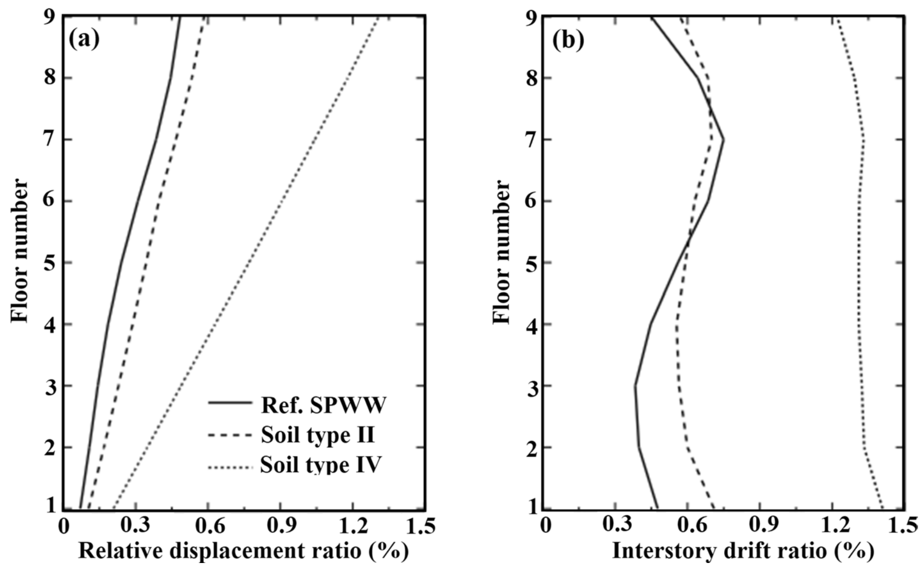

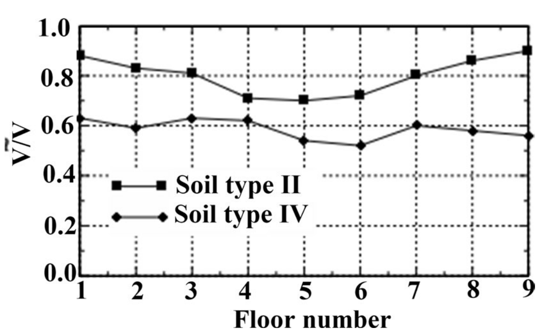

Fig. 12 Ratio of story shear of flexible base to fixed base structure on soil types II and IV

related to its lower floor is due to two factors. The first factor is the story shear force, and the second is the base or foundation rocking motion. It seems that maybe a significant part of the story displacement or drift in a soil–structure system is from base rotation (rocking motion).

In practice, the story drift is calculated by subtracting the horizontal displacement of lower floor from that of upper floor of the story. Thus, for a fixed-base building structure, the horizontal displacement of a floor is measured by only horizontal movement of that floor related to lower floor induced by story shear; that is expressed by parameter $u(t)$ $u(t)$ in Fig. 13a, whereas for a flexible base building structure, the horizontal displacement of a floor is measured by summation of $u(t)u(t)$ (Fig. 13b) due to story shear, and the horizontal movement of the floor related to lower floor produced by the base rotation, which is quantified by $h\theta(t)$ (Fig. 13b), where h is the story height and $\theta(t)$ $\theta(t)$ is the angle of rotation of the lower story floor.

In this study, the total story displacements of the SPSW resting on flexible foundation are decomposed into two

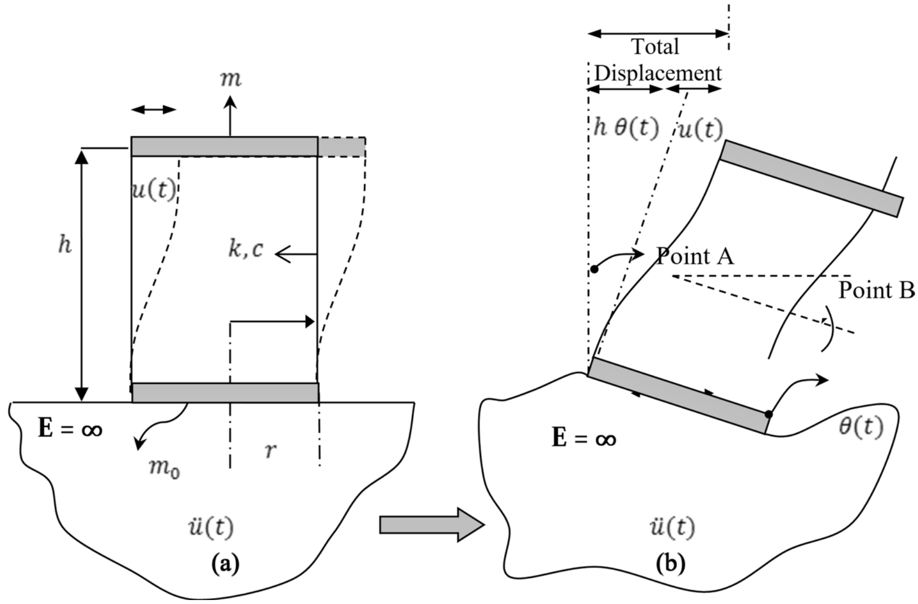

Fig. 13 Displacements of a structural frame with **a** fixed base; and **b** flexible base idealization

displacements including the horizontal movement induced by story shear and the movement produced by base rotation. To achieve *hθ(t)* firstly, the maximum rotation *(θ)* of the SPSW foundation should be defined. This rotation can be calculated as below:

$$\tan(\theta(t)) = \frac{(V_B - V_A)}{2r} \tag{3}$$

where V_A and V_B represent the time histories of vertical displacement of points A and B, respectively, and r is the foundation length (Fig. 13a).

Time history of foundation rotation of SPSW resting on both soil types is shown in Fig. 14. As shown in Fig. 14, peak rotation of foundation attains larger values in the case of soft soil than that of stiff soil.

Now, with subtracting the movement produced by base rotation *hθ(t)* from the total displacement (obtained from time history analysis) of each floor relative to the foundation, it is possible to obtain the story drift due to only story shear. This part of displacement is a movement which is only exerted by story shear, thus it can be calculated in accordance with the following equation:

$$\Delta'_i = \Delta_i - h_i \tan(\theta) \tag{4}$$

where Δ'_i is the story displacement of ith floor relative to the foundation in the absence of foundation rocking effect, Δ_i is

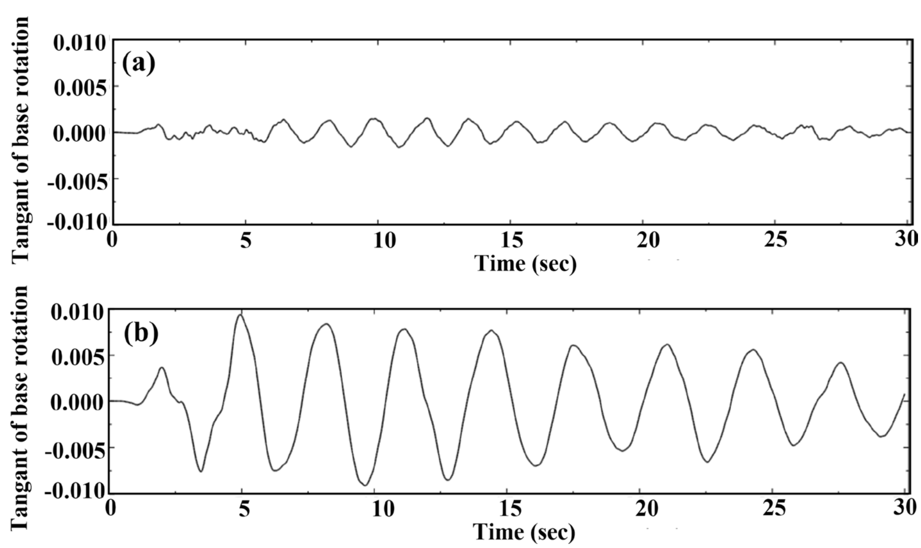

Fig. 14 Time history of foundation rotation of SPSW resting on **a** soil type II and **b** soil type IV

the total displacement of ith floor relative to the foundation obtained from time history analysis, and hi is the height of ith floor relative to the foundation.

Hence, the story drifts of SPSW resting on flexible foundation without any rocking effect (termed as "real story drift" for brevity) can be calculated by following equation;

$$(drift)_i = \left(\Delta'_i - \Delta'_{i-1}\right) \quad (4)$$

where $(drift)_i$ is the story drift of ith floor without rocking motion (real story drift). Figure 15 shows the real story drifts (without considering the rocking motion) for both soil types. It is clear from Fig. 15 that rotation of foundation has much more effect on SPSW resting on soft soil than it does in the case of stiff soil.

A comparison is also presented in Fig. 16 between story drifts of Ref. SPSW [23], and real story drifts of flexible base SPSW computed by the means of Eq. 4. The comparison is overall reasonable indicating that story drifts of Ref. SPSW is always less than real story drifts of SPSW on both soil types.

Comparing this result with the change of story shear clearly demonstrates that real story drifts appear to decrease with decreasing story shear forces due to soil flexibility. Such evidence suggests that story shear has a good compatibility with real story drifts. Moreover, rocking motion of the foundation and the associated increase in response are extremely sensitive to structure height and obviously quite important for high-rise structures rather than low-rise structures. It is an observation supported by proposition in pioneering literature by Veletsos and Meek (1974). Similarly, in the case of low-rise buildings the movement produced by rocking motion has an inconspicuous role in composing total displacement. Therefore, total displacement of stories in these kinds of buildings are generally much closer to real story drifts than the one obtained from high-rise building behavior. It also may be the reason of having lesser story drifts in low-rise buildings due to SSI effects with respect to fixed-base consideration reported by Tabatabaiefar and Massumi (2010), while such response was found to be quite increased in high-rise buildings due to SSI effects.

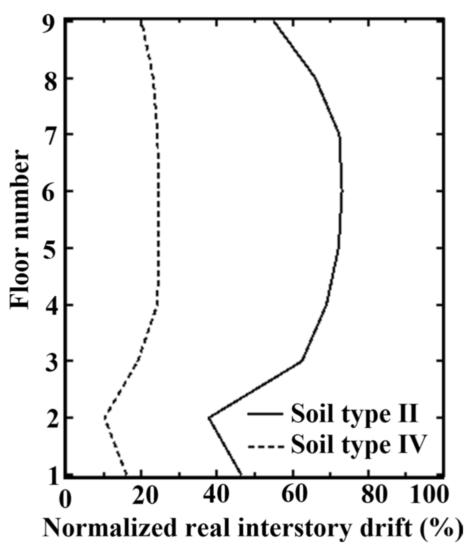

Fig. 15 Real story drift (normalized by the total story drift) over height of the SPSW structure

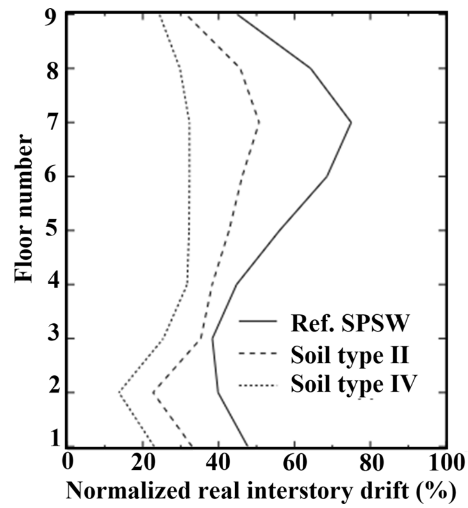

Fig. 16 Real story drift ratios for fixed and flexible base SPSW

It should be noted that the focus of this research is on how the mechanism of the effect of rocking motion on the structural response of a mid-rise SPSW. However, in order to reach a general engineering judgment of the SPSW behavior that includes the SSI effect, it is necessary to perform structural analysis under at least seven different earthquakes, according to ASCE Code. In addition, since the present study dedicates to the mid-rise structure, a further study is recommended to perform on low- and high-rise SPSW structures. More research performed by the authors on the SSI effects on different multi-story SPSWs under different earthquakes can be found in Memarzadeh et al. (2011).

8 Conclusion

This study highlights the importance of nonlinear SSI and its impact on seismic behavior of a mid-rise SPSW. For this purpose, a time direct method was used considering nonlinear behavior of SPSW and using an equivalent-linear model for underneath soil deposit during time history analyses. Two soil types were considered: type II and type IV, corresponding to firm and soft soil deposits, respectively.

The seismic responses of structure were evaluated and compared to those obtained as a fixed base model. In addition, a procedure was presented to clarify how SPSW behavior can be influenced by rocking component. The study revealed that the effect of SSI appreciably alters the seismic response of SPSW. The following observations are obtained:

- Flexibility of soil causes an overall decrease in lateral stiffness resulting in the lengthening of lateral natural periods. It is observed that first four frequencies decrease with increasing soil softness.
- The results showed that the incorporation of SSI tends to decrease story shear of SPSW by reducing the shear wave velocity of the soil deposit. This concept is in agreement with common assumptions, postulated by almost all the design codes.
- A significant increase in structural deflection was observed as a consequence of soil-flexibility. The story drift of SPSW was also found to be influenced by the SSI which generally results in significantly greater story drifts due to the foundation rocking motion particularly in the case of soil type IV.
- While SSI caused increase in total story drifts, the results revealed a decrease in real story drifts due to soil flexibility. Both structure height and softening of soil have the same effect on SPSW behavior due to rocking motion.
- The strong side of the proposed methodology is that it proves that increasing the total drift of the structural layers due to rocking motion has no practical effect on the increase of design forces because in practice the actual drifts are reduced.
- As a weak side of the rocking motion of structures, it causes the well-known P-Delta effect that results in an increase of the overturning moment and needs to be checked, especially for the high-rise buildings.

Author contributions JM, PM contributed to the literature search and review, structure analysis, content planning and manuscript writing. FB was involved in the literature search and review, soil analysis, manuscript writing, editing and proofing. MB helped in the literature search and review, manuscript writing, editing and proofing.

Funding No fund was received for this project.

Data availability No data, models, or code was generated or used during the study.

Declarations

Conflict of interest The authors declare no competing interests.

References

Abkar G, Lorki AA (2011) Evaluation of progressive collapse in steel structures designed based on iranian code of practice for seismic resistant design buildings (Standard No. 2800), 4th Edition and Iranian National Building Code (INBC), Part 10. J Civ Eng Mater Appl is Publ by Raika Pajuhesh Pars 2:192–200

AISC 341-10 - American Institute of Steel Construction (2010) Seismic Provisions for Structural Steel Buildings

ASCE-7 (2000) Minimum design loads for buildings and other structures. American Society of Civil Engineers, Reston, VA

Bahuguna A, Firoj M (2021) Nonlinear seismic performance of nuclear structure with soil–structure interaction. Iran J Sci Technol - Trans Civ Eng. https://doi.org/10.1007/s40996-021-00728-2

Bai J, Zhang J, Jin S et al (2021) A multi-modal-analysis-based simplified seismic design method for high-rise frame-steel plate shear wall dual structures. J Constr Steel Res 177:106484. https://doi.org/10.1016/j.jcsr.2020.106484

Behnamfar F, Banizadeh M (2016) Effects of soil–structure interaction on distribution of seismic vulnerability in RC structures. Soil Dyn Earthq Eng 80:73–86. https://doi.org/10.1016/j.soildyn.2015.10.007

Carbonari S, Dezi F, Leoni G (2008) Soil–structure interaction in the seismic response of coupled wall-frame structures on pile foundations. AIP Conf Proc 1020:610–617. https://doi.org/10.1063/1.2963891

Çelebi E, Göktepe F, Karahan N (2012) Non-linear finite element analysis for prediction of seismic response of buildings considering soil–structure interaction. Nat Hazards Earth Syst Sci 12:3495–3505. https://doi.org/10.5194/nhess-12-3495-2012

Choudhury D, El-zahaby KM, Idriss I (2019) Dynamic soil–structure interaction for sustainable infrastructures. Springer, Cham

Dicleli M, Karalar M (2009) Performance based design of seismic isolated bridges in near-fault zones using elastic-gap devices. In: TCLEE 2009: lifeline Earthquake Engineering in a Multihazard Environment. American Society of Civil Engineers, p 2

Dutta SC, Bhattacharya K, Roy R (2004) Response of low-rise buildings under seismic ground excitation incorporating soil–structure interaction. Soil Dyn Earthq Eng 24:893–914. https://doi.org/10.1016/j.soildyn.2004.07.001

Edip K, Garevski M, Sheshov V, Bojadjieva J (2017) Boundary effects in simulation of soil–structure interaction problems. Soil Mech Found Eng 54:239–243. https://doi.org/10.1007/s11204-017-9464-2

El Ganainy H, El Naggar MH (2009) Seismic performance of three-dimensional frame structures with underground stories. Soil Dyn Earthq Eng 29:1249–1261. https://doi.org/10.1016/j.soildyn.2009.02.003

Ghandil M, Behnamfar F (2017) Ductility demands of MRF structures on soft soils considering soil–structure interaction. Soil Dyn Earthq Eng 92:203–214. https://doi.org/10.1016/j.soildyn.2016.09.051

Gharad AM, Sonparote RS (2019) Study of direct finite element method of analysing soil–structure interaction in a simply supported railway bridge subjected to resonance. Iran J Sci Technol Trans Civ Eng 43:273–286

Herrmann H, Bucksch H (2014) Soil Mechanics and Foundation Engineering. In: Dict. Geotech. Eng. Geotech.

Hökelekli E, Al-Helwani A (2020) Effect of soil properties on the seismic damage assessment of historical masonry minaret–soil interaction systems. Struct Des Tall Spec Build 29:e1694. https://doi.org/10.1002/tal.1694

Homaei F, Yazdani M (2020) The probabilistic seismic assessment of aged concrete arch bridges: the role of soil–structure interaction. Structures 28:894–904. https://doi.org/10.1016/j.istruc.2020.09.038

Jayalekshmi BR, Chinmayi HK (2016) Effect of soil stiffness on seismic response of reinforced concrete buildings with shear walls. Innov Infrastruct Solut. https://doi.org/10.1007/s41062-016-0004-0

Jiao C, Wu R, Long P, Lu Z (2021) A study on seismic behavior of abutments considering soil structure interaction

Kamgar R, Babadaei Samani MR (2022) Numerical study for evaluating the effect of length-to-height ratio on the behavior of concrete frame retrofitted with steel infill plates. Pract Period Struct Des Constr 27:04021062. https://doi.org/10.1061/(asce)sc.1943-5576.0000632

Kamgar R, Gholami F, Zarif Sanayei HR, Heidarzadeh H (2020) Modified tuned liquid dampers for seismic protection of buildings considering soil-structure interaction effects. Iran J Sci Technol - Trans Civ Eng 44:339–354. https://doi.org/10.1007/s40996-019-00302-x

Kamgar R, Tavakoli R, Rahgozar P, Jankowski R (2021) Application of discrete wavelet transform in seismic nonlinear analysis of soil–structure interaction problems. Earthq Spectra 37:1980–2012. https://doi.org/10.1177/8755293020988027

Kamgar R, Askari Dolatabad Y, Babadaei Samani M (2019) Seismic optimization of steel shear wall using shape memory alloy

Kramer SL (1996) Geotechnical earthquake engineering. Prentice Hall Upper Saddle River, New Jersey

Liang J, Han B, Todorovska MI, Trifunac MD (2018) 2D dynamic structure–soil–structure interaction for twin buildings in layered half-space II: incident SV-waves. Soil Dyn Earthq Eng 113:356–390. https://doi.org/10.1016/j.soildyn.2018.05.023

Liu JL, Xu LH, Li ZX (2020) Experimental study on component performance in steel plate shear wall with self-centering braces. Steel Compos Struct 37:341–351. https://doi.org/10.12989/scs.2020.37.3.341

Liu S, Li P, Zhang W, Lu Z (2020b) Experimental study and numerical simulation on dynamic soil–structure interaction under earthquake excitations. Soil Dyn Earthq Eng. https://doi.org/10.1016/j.soildyn.2020.106333

Lysmer J, Kuhlemeyer RL (1969) Finite dynamic model for infinite media. J Eng Mech Div 95:859–877. https://doi.org/10.1061/jmcea3.0001144

Madani B, Behnamfar F, Tajmir Riahi H (2015) Dynamic response of structures subjected to pounding and structure–soil–structure interaction. Soil Dyn Earthq Eng 78:46–60. https://doi.org/10.1016/j.soildyn.2015.07.002

Memarzadeh P, Saadatpour MM, Azhari M (2010) Nonlinear dynamic response and ductility requirements of a typical steel plate shear wall subjected to el centro earthquake. Iran J Sci Technol Trans B Eng 34:371–384

Memarzadeh P, Mirlohi J, B F, et al (2011) Seismic response of steel plate shear walls considering soil–structure interaction. In: Proceedings of the 2nd European conference of control, and proceedings of the 2nd European conference on mechanical engineering, pp 107–112

Memarzadeh P (2008) Ductility behavior of a steel plate shear wall by explicit dynamic analyzing. In: 14th world conference on earthquake engineering (14WCEE)

Motallebiyan A, Bayat M, Nadi B (2020) Analyzing the Effects of soil–structure interactions on the static response of onshore wind turbine foundations using finite element method. Civ Eng Infrastruct J 53:189–205. https://doi.org/10.22059/ceij.2020.281914.1586

Oliveto G, Santini A (1993) A simplified model for the dynamic soil–structure interaction of planar frame-wall systems. Eng Struct 15:431–438. https://doi.org/10.1016/0141-0296(93)90061-8

Ordonez GA (2007) SHAK2000 A Computer Program for the 1D Analysis of Geotechnical Earthquake Engineering Problems. geomotions.com

Provisions BP on ISS, Agency USFEM (1997) NEHRP Recommended Provisions for Seismic Regulations for New Buildings and Other Structures: Commentary. Washington, DC Available from www bssconline org/NEHRP2000/comments/provisions/(last accessed December 2004) 9

Raychowdhury P (2011) Seismic response of low-rise steel moment-resisting frame (SMRF) buildings incorporating nonlinear soil–structure interaction (SSI). Eng Struct 33:958–967. https://doi.org/10.1016/j.engstruct.2010.12.017

Rezai M (1999) Seismic behaviour of steel plate shear walls by shake table testing. The University of British Columbia

Sabelli R, Bruneau M (2006) Steel Plate Shear Walls (Steel Design Guide 20). Am Inst Steel Constr Inc

Shabanlou M, Moghaddam H, Saedi Daryan A (2021) The effect of geometry on structural behavior of buildings with steel plate shear wall system subjected to blast loading. Int J Steel Struct 21:650–665. https://doi.org/10.1007/s13296-021-00463-4

Shirzadi M, Behnamfar F, Asadi P (2020) Effects of soil–structure interaction on inelastic response of torsionally-coupled structures. Bull Earthq Eng 18:1213–1243. https://doi.org/10.1007/s10518-019-00747-5

Tabatabaiefar HR, Massumi A (2010) A simplified method to determine seismic responses of reinforced concrete moment resisting building frames under influence of soil–structure interaction. Soil Dyn Earthq Eng 30:1259–1267. https://doi.org/10.1016/j.soildyn.2010.05.008

Tavakoli R, Kamgar R, Rahgozar R (2020) Optimal location of energy dissipation outrigger in high-rise building considering nonlinear soil–structure interaction effects. Period Polytech Civ Eng 64:887–903. https://doi.org/10.3311/PPci.14673

Veletsos AS, Meek JW (1974) Dynamic behaviour of building-foundation systems. Earthq Eng Struct Dyn 3:121–138. https://doi.org/10.1002/eqe.4290030203

Wang W, Luo Q, Sun Z et al (2021) Relation analysis between out-of-plane and in-plane failure of corrugated steel plate shear wall. Structures 29:1522–1536. https://doi.org/10.1016/j.istruc.2020.12.030

White W, Valliappan S, Lee IK (1977) Unified boundary for finite dynamic models. ASCE J Eng Mech Div 103:949–964. https://doi.org/10.1061/jmcea3.0002285